MICROBIOLOGY

All major cholesterol-dependent cytolysins use glycans as cellular receptors

Lucy K. Shewell[1]*, Christopher J. Day[1]*, Freda E.-C. Jen[1], Thomas Haselhorst[1], John M. Atack[1], Josephine F. Reijneveld[1], Arun Everest-Dass[1], David B. A. James[2], Kristina M. Boguslawski[2], Stephan Brouwer[3], Christine M. Gillen[3], Zhenyao Luo[3,4], Bostjan Kobe[3,4], Victor Nizet[5], Mark von Itzstein[1], Mark J. Walker[3], Adrienne W. Paton[6], James C. Paton[6], Victor J. Torres[2], Michael P. Jennings[1]†

Cholesterol-dependent cytolysins (CDCs) form pores in cholesterol-rich membranes, but cholesterol alone is insufficient to explain their cell and host tropism. Here, we show that all eight major CDCs have high-affinity lectin activity that identifies glycans as candidate cellular receptors. Streptolysin O, vaginolysin, and perfringolysin O bind multiple glycans, while pneumolysin, lectinolysin, and listeriolysin O recognize a single glycan class. Addition of exogenous carbohydrate receptors for each CDC inhibits toxin activity. We present a structure for suilysin domain 4 in complex with two distinct glycan receptors, P_1 antigen and αGal/Galili. We report a wide range of binding affinities for cholesterol and for the cholesterol analog pregnenolone sulfate and show that CDCs bind glycans and cholesterol independently. Intermedilysin binds to the sialyl-TF O-glycan on its erythrocyte receptor, CD59. Removing sialyl-TF from CD59 reduces intermedilysin binding. Glycan-lectin interactions underpin the cellular tropism of CDCs and provide molecular targets to block their cytotoxic activity.

INTRODUCTION

The common feature of the cholesterol-dependent cytolysins (CDCs) is the ability to form pores in membranes. The multistep process of pore formation by the CDCs is as follows: Soluble CDC monomers bind to the cellular membrane, the monomers then interact with each other to form an oligomeric prepore structure consisting of 34 to 50 monomers, and then the prepore structure collapses vertically to penetrate into the membrane, becoming a transmembrane β barrel pore (*1*, *2*).

The importance of membrane cholesterol in CDC function has been known since 1939, when it was reported that preincubation of the CDC streptolysin O (SLO; from *Streptococcus pyogenes*) with free cholesterol inhibited hemolytic activity (*3*). Later work with listeriolysin O (LLO; from *Listeria monocytogenes*) showed that preincubation with cholesterol inhibited oligomerization of the toxin in cellular membranes, preventing pore formation and blocking hemolytic and cytolytic activity. However, it is notable that cholesterol does not interfere with membrane binding of LLO or its ability to induce cytokine expression in macrophages (*4*, *5*), indicating that other cellular receptors may exist. Intermedilysin (ILY; from *Streptococcus intermedius*) requires cholesterol for insertion of the pore into the membrane (*6*) but uses human CD59 (hCD59) as a cellular receptor (*7*).

Several proteinaceous receptors for membrane lipid-dependent, pore-forming toxins from *Staphylococcus aureus* have recently been identified (*8*). Furthermore, we have shown that the CDCs SLO and pneumolysin (Ply; from *Streptococcus pneumoniae*) require binding to glycan cellular receptors on red blood cells (RBCs) for hemolytic activity (*9*). In the current study, we examine all major CDCs for glycan binding properties using a comprehensive glycan array and investigate the role of specific glycans as functional cellular receptors for CDCs.

RESULTS

All CDCs screened by glycan array have lectin activity

All major CDCs [Ply, SLO, perfringolysin O (PFO), vaginolysin (VLY), lectinolysin (LLY), LLO, suilysin (SLY), and ILY] were screened for lectin activity using an array of 402 unique glycan structures to identify potential glycan receptors. The His-tagged CDCs were detected with a fluorescent antibody complex. All of the CDCs screened showed glycan binding to a unique set of glycan structures (Fig. 1 and data S1). Some toxins showed highly specific binding; for example, LLY bound a single structure, while other CDCs such as SLO and PFO bound to a broad range of glycans. The binding profile of each CDC is detailed below.

To further investigate the glycan array results using an independent method and to characterize the kinetics of the interactions of the CDCs with their glycan targets, we used surface plasmon resonance (SPR). Recombinant His-tagged CDCs (see Materials and Methods and fig. S1) were immobilized, and free glycans were flowed over the proteins. These data showed high-affinity glycan interactions for all CDCs tested (Table 1 and table S1). CDCs have a conserved, four-domain structure (*10*). Ply binds to its glycan receptor, sialyl-Lewis X (sLex), via domain 4 (D4) (*9*). To investigate whether D4 mediates glycan binding in other CDCs, we expressed and purified D4 of LLO, ILY, and SLY and examined these domains for glycan binding by SPR. The glycan binding we observed with the whole toxins was recapitulated by the recombinant domain 4 from LLO, ILY, SLY, and Ply (*9*) and indicated that glycan binding via D4 may be a common feature of all CDCs (Table 1).

[1]Institute for Glycomics, Griffith University, Gold Coast, QLD 4222, Australia. [2]Department of Microbiology, New York University School of Medicine, New York, NY 10016, USA. [3]School of Chemistry and Molecular Biosciences and the Australian Infectious Diseases Research Centre, University of Queensland, Brisbane, QLD 4072, Australia. [4]Institute for Molecular Bioscience, University of Queensland, Brisbane, QLD 4072, Australia. [5]Department of Pediatrics and Skaggs School of Pharmacy and Pharmaceutical Sciences, University of California, San Diego, La Jolla, CA 92093, USA. [6]Research Centre for Infectious Diseases, Department of Molecular and Biomedical Science, University of Adelaide, Adelaide 5005, Australia.
*These authors contributed equally to this work.
†Corresponding author. Email: m.jennings@griffith.edu.au
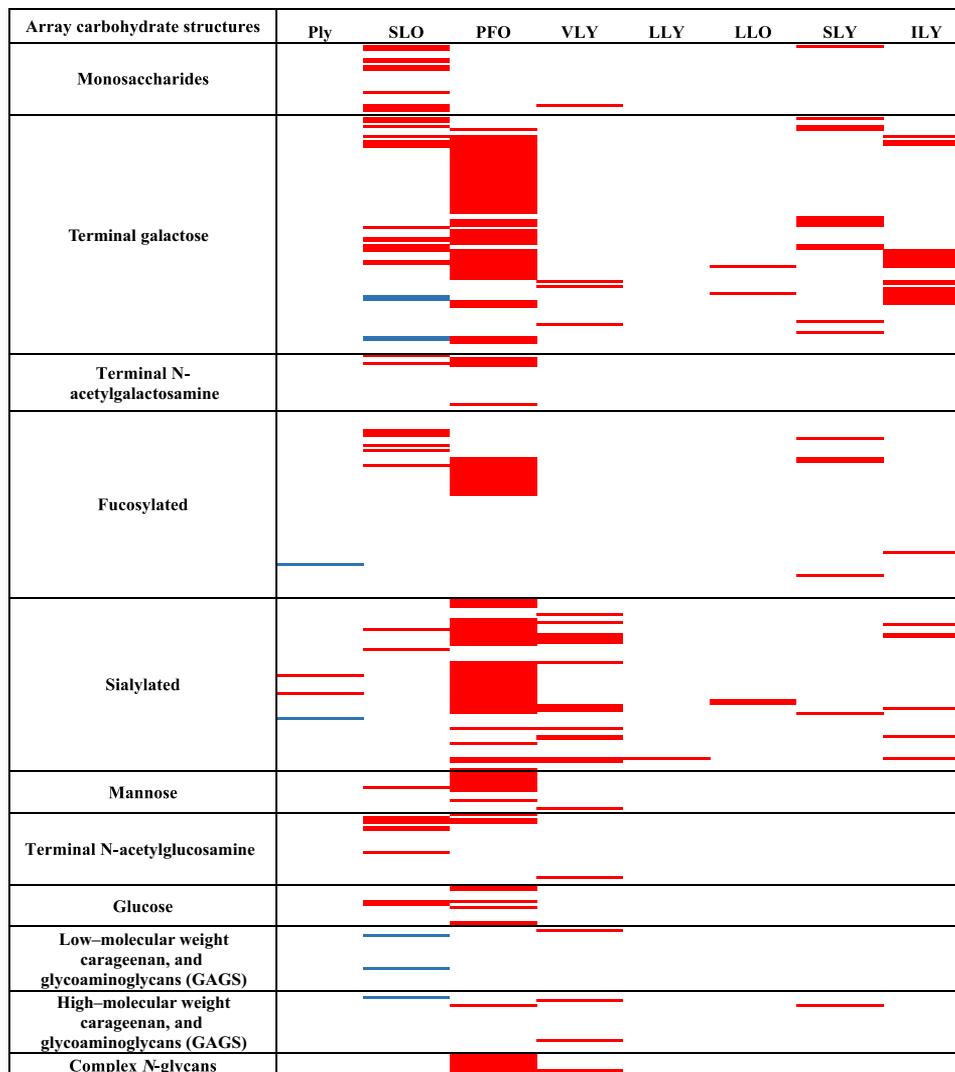
Fig. 1. Glycan array analyses of glycan binding by CDCs. Red indicates binding above background. Blue indicates binding observed here and previously (*9*). White indicates that the structure was not bound. Classes of glycans arrayed are indicated to the left of the figure. A complete list of glycan structures on the array and the mean fold fluorescence increase above background of three replicate glycan array experiments are shown in data S1. GAGs, glycosylaminoglycans.

SLO: Human blood group B antigen type IV pentasaccharide can inhibit SLO hemolytic activity

SLO is a major virulence factor of group A *Streptococcus* (*S. pyogenes*) (*11*). Although SLO bound to a broad range of glycans in the array studies, SPR analysis showed that the highest affinity interactions were detected for the ABO blood group antigens, with the highest affinity observed for the group B type IV pentasaccharide with a dissociation constant (K_D) of 116 pM (Table 1), several fold higher than the previously identified ligand, lacto-*N*-neotetraose (*9*).

We next investigated whether these high-affinity glycan ligands could inhibit SLO hemolytic activity. SLO lysis of human RBCs was assessed in the presence of three of the synthetic ABO blood group antigen structures (Fig. 2A). Despite the broad range of glycan binding we observed with SLO on the glycan array, the blood group B type IV pentasaccharide was able to completely inhibit SLO hemolytic activity, consistent with a single glycan binding site on SLO. Differential blood group antigen inhibition of SLO hemolytic activity was in proportion to the binding affinities determined by SPR (Fig. 2A).

We investigated the susceptibilities of the different human blood groups to SLO, but we did not observe any obvious differences in the hemolytic activity of SLO against human groups O, A, and B RBCs. The blood group B type IV antigen has not been detected on RBCs from group B donors (*12*), which would explain this observation. There may be other cell types with high levels of the blood group B type IV antigen that are highly sensitive to SLO-mediated cytolysis.

PFO: PFO has broad lectin activity, with a preference for structures containing the sialic acid, Neu5Ac

PFO is one of two toxins produced by *Clostridium perfringens* that are considered to be essential for the development of gas gangrene in humans (*13*). However, paradoxically, PFO is not essential for disease in a mouse model (*14*). As the receptor biology of PFO is not well understood, it is not known whether the human-specific role for PFO in disease is due to differences in receptor expression. Glycan array analysis showed that PFO bound to a broad range of glycans

Table 1. A subset of SPR results for CDCs against glycans plus cholesterol and PS. Glycans, cholesterol, and PS were tested at concentrations listed in data S2 and the Materials and Methods. Data shown are the mean K_{DS} from at least three independently run SPR analyses. NCDI, no concentration dependent binding observed up to the maximum concentration tested; n.t., not tested, sample was not run against that toxin. α1-3Gal tri, Galili (αGa1) antigen trisaccharide; sTF, Neu5Acα2-3Ga1β1-3Ga1NAc; sLeC, Neu5Acα2-3Ga1β1-3G1cNAc; α2-6sLN, Neu5Acα2-6LacNAc; BGA tri, blood group A trisaccharide; BGA type 4, blood group A type IV pentasaccharide; BGB type 4, blood group B type IV pentasaccharide; BGH di, blood group H antigen disaccharide; BGH type 4, blood group H antigen type IV tetraose; PS, pregnenolone sulfate (sodium salt). For the full range of glycans tested, error, and more than two significant figures, see table S1.

	Ply	SLO	PFO	VLY	LLY	LLY (−LD)	LLO	LLO D4	SLY	SLY D4	ILY	ILY D4
GT2	n.t.	NCDI	n.t.	n.t.	n.t.	n.t.	6.7 nM	10 nM	n.t.	n.t.	n.t.	n.t.
α1-3Gal tri	n.t.	n.t.	n.t.	n.t.	n.t.	n.t.	n.t.	n.t.	258 nM	547 nM	NCDI	NCDI
P₁ Antigen	n.t.	n.t.	n.t.	n.t.	n.t.	n.t.	n.t.	n.t.	359 nM	342 nM	NCDI	NCDI
LNnT	n.t.	0.93 nM	2.8 μM	NCDI	NCDI	n.t.	NCDI	NCDI	n.t.	n.t.	4.9 μM	n.t.
TF	n.t.	n.t.	46 μM	n.t.	NCDI	n.t.	n.t.	n.t.	n.t.	n.t.	60 μM	n.t.
sTF	n.t.	n.t.	13 μM	n.t.	NCDI	n.t.	n.t.	n.t.	NCDI	NCDI	599 nM	568 nM
sLeC	n.t.	1.4 μM	1.6 μM	NCDI	16 μM	n.t.	n.t.	n.t.	NCDI	NCDI	16 μM	4.9 μM
α2-6sLN	n.t.	n.t.	23 μM	633 nM	1.6 μM	1.8 μM	n.t.	n.t.	n.t.	n.t.	NCDI	NCDI
sLeX	1.3 μM	3.1 μM	3.9 μM	n.t.	n.t.	n.t.	n.t.	n.t.	NCDI	NCDI	2.8 μM	4.9 μM
BGA tri	n.t.	1.3 μM	5.1 μM	n.t.	NCDI	n.t.	n.t.	n.t.	8.7 nM	4.4 nM	9.9 μM	4.9 μM
BGA type 4	n.t.	105 nM	150 μM	n.t.	NCDI	n.t.	n.t.	n.t.	5.7 μM	9.2 μM	NCDI	NCDI
BGB type 4	n.t.	0.12 nM	32 μM	n.t.	NCDI	n.t.	n.t.	n.t.	8.4 μM	6.4 μM	NCDI	n.t.
BGH di	n.t.	603 nM	NCDI	n.t.	NCDI	n.t.	n.t.	n.t.	19 μM	26 μM	NCDI	NCDI
BGH type 4	n.t.	2.6 μM	NCDI	n.t.	NCDI	n.t.	n.t.	n.t.	n.t.	n.t.	NCDI	NCDI
Cellobiose	NCDI	NCDI	34 μM	NCDI	NCDI	n.t.	NCDI	NCDI	NCDI	NCDI	NCDI	NCDI
Cholesterol	1 μM	189 nM	296 nM	NCDI	NCDI	NCDI	NCDI	NCDI	NCDI	NCDI	NCDI	NCDI
PS	0.4 nM	52 nM	n.t.	n.t.	n.t.	997 nM	n.t.	214 nM	1.8 μM	n.t.	588 nM	NCDI

(Fig. 1), with SPR measurements indicating the highest affinity binding to sialylated structures (Table 1). PFO showed a binding preference to *N*-acetylneuraminic acid (Neu5Ac) sialylated structures compared to *N*-glycolylneuraminic acid (Neu5Gc) sialylated structures. For example, SPR demonstrated that PFO has a 72-fold higher affinity for Neu5Acα2-3Galβ1-3GlcNAc (*N*-acetylglucosamine) (sLeC) than the Neu5Gc equivalent structure (table S1). Humans do not express Neu5Gc on normal tissues due to an inactive CMAH (Cytidine monophosphate-*N*-acetylneuraminic acid hydroxylase) enzyme, therefore a Neu5Ac preference may reflect adaptation to the human host. The type of sialic acid linkage (α2-3 compared to α2-6) also influences binding preference, as PFO had higher affinity for Neu5Acα2-3LeC compared to the corresponding α2-6–linked structure (Table 1). Overall, sLeC was the highest affinity PFO glycan ligand identified in our SPR analysis. The presence of 2 mM sLeC significantly inhibited PFO hemolytic activity (Fig. 2B), suggesting a role for glycan binding on the RBC surface in mediating PFO hemolytic activity.

VLY: VLY hemolytic activity can be inhibited with the glycan Neu5Acα2-6LacNAc

VLY is the CDC produced by *Gardnerella vaginalis*, a facultative anaerobic bacterium found in most of women with bacterial vaginosis. VLY is one of the few known virulence factors of *G. vaginalis* (*15*). Like SLO and PFO, VLY is bound to a broad range of glycans (Fig. 1). SPR analysis confirmed an interaction between VLY and the glycan

Neu5Acα2-6LacNAc, with a K_D of 633.4 nM (Table 1). The presence of 100 μM Neu5Acα2-6LacNAc inhibited the hemolytic activity of VLY against human RBCs (Fig. 2C).

LLY: LLY binds to a single glycan

Streptococcus mitis produces the CDC LLY, also referred to as human platelet aggregation factor. In addition to the four-domain structure that is common to CDCs, LLY has an extra 162–amino acid N-terminal lectin domain (*16*). This N-terminal lectin domain was reported to have specificity for Lewis Y and Lewis B glycans; this specificity was demonstrated by probing a glycan microarray with a fluorescently labeled version of the LLY lectin domain in the absence of LLY domains 1 to 4 (*17*). We analyzed the full-length His-tagged LLY and found that, unlike the other CDCs, LLY only bound to a single glycan structure on the array (Fig. 1).

SPR analysis showed that LLY can bind to the terminal structure of this biantennary glycan, Neu5Acα2-6LacNAc, and to sLeC, which has the same structure but with an α2-3–linked terminal Neu5Ac (Table 1). LLY hemolytic activity was inhibited with 2 mM sLeC (Fig. 2D). SPR analysis was also performed with LLY lacking the N-terminal lectin domain, LLY-LD. This protein recapitulated full-length LLY binding to Neu5Acα2-6LacNAc, confirming that the previously identified N-terminal lectin domain has no role in the lectin activity observed here. Consistent with our observation, removal of the N-terminal lectin domain from LLY does not considerably alter the hemolytic activity of this toxin (*17*), and the species-dependent hemolytic activity is dictated by D4 of LLY (*18*).
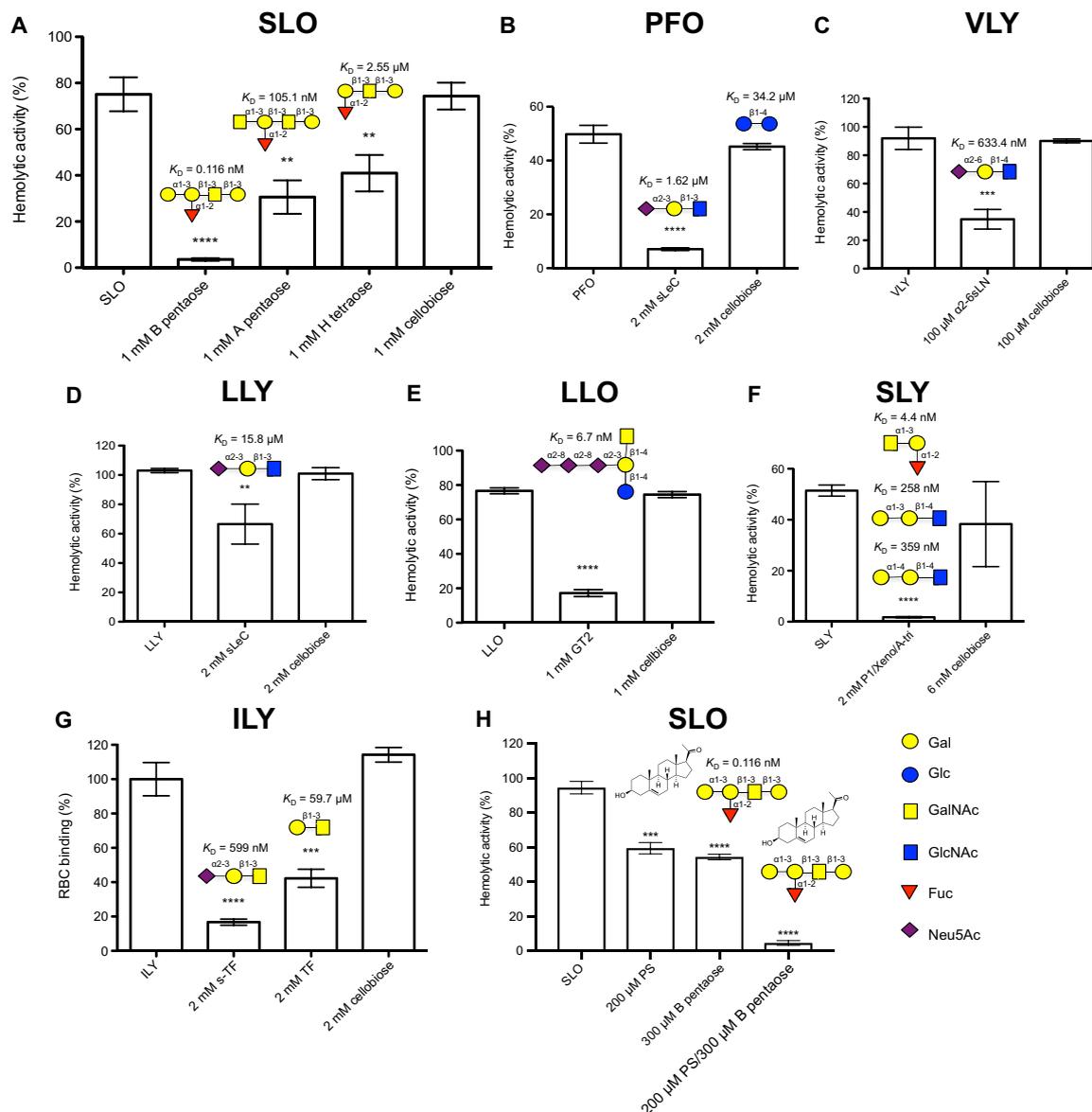
Fig. 2. Analysis of the hemolytic activity of CDCs in the presence of candidate glycan cellular receptors. (**A** to **F**) The hemolytic activity of the CDCs at the hemolytic dose 100 (HD$_{100}$) or HD$_{50}$ against 1% (v/v) human group O RBCs was determined after preincubation with phosphate-buffered saline, or with the indicated concentration of candidate glycan receptor, or with the same concentration of cellobiose, which served as a common, nonbinding glycan control. For the analysis of the impact of sTF and TF on ILY binding to RBCs (**G**), RBCs were fixed to the wells of a 96-well plate, and the ability of 2 mM sTF, 2 mM TF, or 2 mM cellobiose to block the binding of 25 ng of ILY was assessed. The HD$_{100}$ of SLO was also assessed in the presence of blood group B type IV pentasaccharide and pregnenolone sulfate (PS) (sodium salt) (**H**), individually and in combination (see fig. S7G for determination of HD$_{100}$ of SLO and fig. S7, I and J for hemolytic assays in the presence of a range of concentrations of blood group B type IV pentasaccharide and PS). Results presented are a representative assay conducted with a single blood donor and are shown as the mean of triplicate samples, with error bars showing ±1 SD from the mean. Multiple independent assays (minimum of three) were performed all showing the same trend. The percentage values for each data point used to generate bar graphs are shown in table S4A. The structure of the glycan receptor and the K_D of the CDC for the glycan as determined by SPR are shown above the appropriate bar in each histogram. Statistical significance was determined using a two-tailed unpaired Student's t test. **$P < 0.005$, ***$P < 0.0005$, and ****$P < 0.0001$. P values for t tests comparing hemolytic activity of CDCs without and with glycan/PS are shown in table S4B. B pentaose, blood group B type IV pentasaccharide; A pentaose, blood group A type IV pentasaccharide; H tetraose, blood group H antigen type IV tetraose; sLeC, sialyl-Lewis C; α2-6SLN, Neu5Acα2-6 LacNAc; P1, P$_1$ antigen; Xeno, Xeno antigen/Galili epitope; A-tri, blood group A trisaccharide; sTF, sialyl-TF.

LLO: LLO binds to carbohydrate structures found on the C-series gangliosides

LLO is an essential virulence factor produced by the intracellular pathogen *L. monocytogenes* (*19*). LLO is unique among the CDCs, as it displays pH-dependent behavior, with maximal hemolytic and cytolytic activity at pH 5.5 (*20*). Glycan array analysis with LLO re-

vealed binding to the C-series ganglioside structures. We assessed the glycan binding of LLO at pH 7.0 and 5.5 and found that interactions with the C-series ganglioside structures were pH dependent (Table 1 and table S1). The highest affinity LLO ligand is the glycan structure found on the C-series ganglioside GT2 at pH 5.5. The correspondence of the pH optima of LLO cytolytic activity with the

highest binding affinity for the glycan receptor identified in this study supports the role of engagement of LLO with these receptors to potentiate cytolytic activity. Free GT2 glycan blocked LLO-mediated hemolytic activity against human RBCs (Fig. 2E), and flow cytometry analysis of LLO binding showed that 2 mM free GT2 inhibited association of the toxin with the RBC surface (fig. S2, A and B). These data are consistent with previous studies on SLO and Ply (9), indicating that blocking access to cellular glycan receptors prevents CDCs binding to the target cell surface.

SLY: SLY engages structurally distinct glycan receptors via multiple glycan binding sites

Streptococcus suis is a major swine pathogen and causes a variety of diseases. It is also recognized as an emerging human pathogen, particularly in Southeast Asia, where it is a primary cause of bacterial meningitis. *S. suis* produces the CDC SLY (21).

Glycan array analysis of SLY showed binding to both terminals α1-3 and α1-4 Gal structures lacking a branched fucose moiety (Fig. 1). SPR analysis of SLY revealed high-affinity binding to Galα1-3Galβ1-4GlcNAc (αGal/Galili epitope, nonhuman), to the human P blood group antigen P_1, and to the human ABO blood group A trisaccharide (Table 1). The αGal/Galili epitope is abundantly expressed on glycoconjugates of nonprimate mammals, including pigs, and is not expressed in humans, apes, and Old World monkeys. Antibodies against the αGal epitope are the most abundant naturally occurring antibodies in humans and are responsible for xenograft rejection of pig organs in humans (22). SPR analysis of purified D4 of SLY showed that all lectin activity resided in D4 (Table 1).

Blocking of SLY hemolytic activity was attempted using three distinct high-affinity glycan ligands. Individually or in combinations of two, these glycans did not inhibit SLY hemolytic activity when tested up to 2 mM. However, a combination of all three glycans at 2 mM completely blocked SLY hemolytic activity against human RBCs (Fig. 2F). These findings suggest that SLY may have multiple binding sites that correspond to these structurally distinct (see Fig. 2F) glycan receptors.

Ply: sLeX glycosylated Mac-1 is a cellular receptor for Ply on human phagocytes

sLeX is a cellular receptor for Ply on human RBCs (9). Others report mannose as a receptor and a crystal structure of Ply with monosaccharide mannose has been reported (23). We did not observe mannose as a high-affinity ligand for Ply (K_D = 338 mM; table S1). In previous work, we demonstrated that Ply cytotoxicity for human phagocytic cells could not be blocked with exogenous sLeX (9) and hypothesized the potential for alternative receptors. *S. aureus* toxin LukAB uses the I-domain of the CD11b component of Mac-1 (Macrophage-1 antigen) as a cellular receptor (24). The I-domain of human CD11b has a single glycosylation: an *N*-linked glycan terminating in sLeX (25). We hypothesized that Ply may also engage glycosylated CD11b as a cellular receptor and used SPR analysis with Ply flowed over immobilized human Mac-1. Ply has a high-affinity interaction with Mac-1 (K_D = 6.62 nM) (Fig. 3A). When the sLeX *N*-glycan of Mac-1 (fig. S3) was enzymatically removed, the affinity of Ply for Mac-1 was reduced approximately fourfold (K_D = 27.8 nM; Fig. 3A), indicating a key role for the glycan in the Ply-receptor interaction. Ply interaction with unglycosylated recombinant human I-domain was not significantly different from deglycosylated Mac-1 (K_D = 22.3 nM, P = 0.4013; Fig. 3A), demonstrating the I-domain mediates the polypeptide interaction with Ply. To confirm the role of CD11b as a receptor for Ply in the intoxication of human phagocytic cells, *S. pneumoniae* express-

ing either wild-type Ply or a mutant, nontoxic version of Ply (Ply L460D) were tested for cytotoxicity against THP-1 cells with and without short hairpin RNA (shRNA) knockdown of CD11b expression. The reduction in surface expression of CD11b on THP-1 cells has been confirmed by flow cytometry (26). We observed a ~30% reduction in cytotoxicity with the pneumococcus expressing wild-type Ply when CD11b was knocked down in THP-1 cells (Fig. 3B). There was no cytotoxicity observed for the Ply L460D mutant strain (Fig. 3B), indicating that the effect we observed by knocking down CD11b was Ply-dependent.

ILY: *O*-linked glycans are crucial components of the CD59 receptor for ILY on human erythrocytes

ILY is a major virulence factor for *S. intermedius*, a causative agent of brain and liver abscesses in humans (27). ILY uses the ~20 kDa glycophosphatidyl-inositol (GPI)–anchored membrane glycoprotein hCD59 as a receptor. hCD59 has a single *N*-glycosylation site (Asn18) and multiple *O*-glycosylation sites (28). Glycan array analysis identified ILY binding to the glycan structure Neu5Acα2-3Galβ1-3GalNAc, also known as sialyl-TF (Thomsen–Friedenreich) (sTF; Fig. 1), one of the most abundant *O*-linked glycans present on human erythrocyte CD59 (28). These findings prompted us to investigate whether sTF on hCD59 was contributing to the interaction of ILY with this cellular receptor.

SPR analysis showed that the K_D of the interaction between ILY and sTF was 599 nM (Table 1). ILY also bound to the asialo version of sTF (TF). The affinity of ILY for TF was almost 100-fold lower than for sTF, indicating that the sialic acid residue of sTF is important for ILY binding. Moreover, the recognition of sialic acid–terminated structures by ILY showed a marked preference for Neu5Ac over Neu5Gc, indicating human adaptation of this CDC (table S1). We found that recombinant D4 of ILY recapitulated the lectin activity of full-length ILY (Table 1). We observed that sTF can significantly inhibit the binding of ILY to human RBCs (Fig. 2G), showing that this *O*-linked glycan is crucial in hCD59's role as a cellular receptor for ILY.

Previous studies have shown that the *N*-linked glycan on hCD59 is not involved in the binding of ILY (7), and our studies here confirm these findings (fig. S4A). To further investigate the role of the *O*-linked sTF on hCD59 in ILY binding, we treated solubilized RBC membrane proteins with α2-3 neuraminidase to remove the sialic acid from sTF or with both α2-3 neuraminidase and *O*-glycosidase to remove the entire sTF structure from hCD59. The untreated and treated RBC membrane proteins were probed with ILY labeled with biotin (Fig. 4 and fig. S4B). We found that the removal of the sialic acid from the *O*-linked glycan or removal of the entire *O*-linked glycan from hCD59 reduced the binding of ILY, indicating that *O*-linked sTF is a crucial component of this glycoprotein receptor for ILY.

The structural basis of CDC-glycan receptor interactions

X-ray crystal structures are available for all CDCs investigated in this study [reviewed in (29)]. To identify the structural basis of glycan binding to the CDCs observed in our analyses, crystal soaks and cocrystallization studies were attempted with the highest affinity ligands in Table 1. No cocrystals could be obtained, and crystal soaks resulted in no obvious glycan binding. All high-affinity glycan binding observed in SPR analysis is via D4 of the CDCs tested (Table 1). We purified D4 from multiple toxins (Ply, LLO, ILY, SLO, and SLY) to attempt nuclear magnetic resonance (NMR) as an alternative approach to study the CDC-glycan interactions. Only D4 of SLY was sufficiently soluble for assignment of the two-dimensional (2D) spectra.

A

	Mac-1	Mac-1 + PNGase	I-domain
Ply	6.62 nM ± 0.9	27.8 nM ± 9.2	22.3 nM ± 4.3
Anti-sLeX	3.865 nM ± 1.307	NCDI	NCDI

B
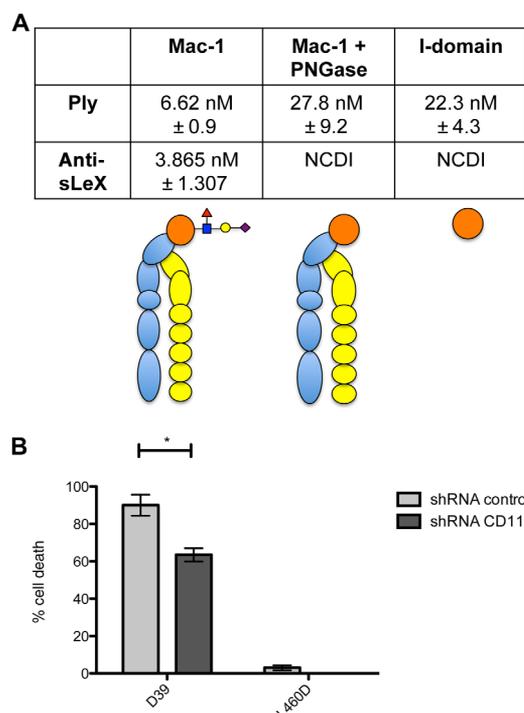
Fig. 3. Analysis of the interaction of Ply with sLeX-glycosylated Mac-1 and cytotoxicity for THP-1 cells with and without CD11b. (**A**) SPR measurements for the affinity of Ply for Mac-1, Mac-1 with the *N*-linked sLeX glycan removed using peptide *N*-glycosidase (PNGase) (Mac-1 + PNGase), and the CD11b I-domain showing sLeX enhanced binding to Mac-1 ($P = 0.0163$) and that glycan-independent binding of Ply to Mac-1 occurs via the I-domain as no difference in binding was observed between Mac-1 lacking sLeX and recombinant human I-domain ($P = 0.4031$). NCDI, no concentration dependent interaction detected at the concentrations tested. A graphical representation of the Mac-1 complex is shown under the SPR K_D values: CD18 = yellow, CD11b = blue, and I-domain = orange, with sLeX glycosylation of I-domain structure shown. (**B**) Cytotoxicity of *S. pneumoniae* D39 expressing wild-type Ply (D39) or a nontoxic version of Ply (Ply460D and L460D) for THP-1 cells with control shRNA (shRNA control) or THP-1 CD11b shRNA knockdown cells (shRNA CD11b). A multiplicity of infection of 2.5 of *S. pneumoniae* cells was used. Results are shown as the mean of duplicate, independent assays (each assay consisting of triplicate samples), with error bars showing ±1 SD from the mean. Statistical significance was determined using a two-tailed unpaired Student's *t* test. *$P < 0.05$.

SLY: Monitoring the binding of two glycan receptors to SLY D4 with ^{1}H-^{15}N HSQC NMR experiments

To study the binding interaction between SLY D4 and the αGal/Galili epitope and the P$_1$ antigen, initially, the backbone chemical shifts (^{1}H$_N$, ^{15}N, ^{13}C$_\alpha$, and ^{13}C$_\beta$) of the SLY D4 protein were assigned (fig. S5 and table S2) using double-labeled (^{13}C/^{15}N) protein and triple resonance NMR experiments. Then, we monitored the binding of the αGal/Galili epitope and the P$_1$ antigen to SLY D4 using ^{1}H-^{15}N heteronuclear single quantum coherence (HSQC) NMR spectroscopy in the presence of ligands shown in Fig. 5. The spectrum of SLY D4 in complex with the αGal/Galili epitope (Fig. 5A) revealed substantial signal intensity changes for Arg[465] and Asp[469] compared to the uncomplexed *apo*-SLY D4 spectra, suggesting that this glycan binds to a high-affinity site with a slow off rate (*30*). In addition, ^{15}N and ^{1}H chemical shift perturbations (CSPs) were observable for Ala[398] and Asp[394], suggesting a lower affinity binding site with a faster off rate. ^{1}H-^{15}N HSQC NMR spectra of SLY D4 in complex with P$_1$ antigen (Fig. 5B) revealed signal intensity changes for Asp[394] and Ser[396],
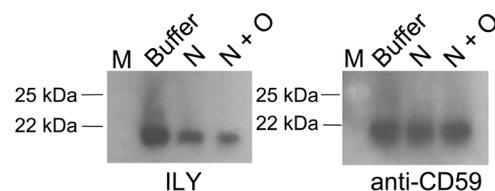
Fig. 4. Analysis of the impact, on ILY binding, of removing the sialic acids and *O*-linked glycans from RBC hCD59. Solubilized RBC membrane proteins were treated with α2-3 neuraminidase (N) to remove the sialic acids from hCD59, or with both α2-3 neuraminidase and *O*-glycosidase (N + O) to remove *O*-linked glycans from hCD59, or with enzyme buffer only under the same conditions (buffer); then were probed with biotin labeled ILY (ILY). Western blotting with anti-CD59 polyclonal antibody confirmed that ILY was binding to hCD59 (anti-CD59). M, molecular weight marker. See fig. S4B for complete far Western/Western blot images and Coomassie-stained gel.

also suggesting a high-affinity site and slow off rate. No CSPs were observed in the SLY D4/P$_1$ antigen complex HSQC spectra. Control NMR experiments with cellobiose, a nonbinding glycan, showed neither CSPs nor signal intensity changes (fig. S6A). Our NMR results of the ^{1}H-^{15}N HSQC titration experiments (Fig. 5, A and B) are in excellent agreement with an unbiased molecular docking study of αGal/Galili that identified a potential αGal-specific binding site. The Galili epitope and the P$_1$ antigen were both docked into the two potential sites. Arg[465]/Asp[469] and Asp[394]/Ser[396] were identified as potential αGal binding sites with high ligand occupancy (Fig. 5C). The methyl protons of the *N*-acetamido group of the reducing GlcNAc residue are involved in strong hydrophobic interactions with the Asp[469]. Similarly, the C6 of GlcNAc with two geminal protons (H6 and H6′) are engaging hydrophobically with Thr[466]. Arg[465] plays a crucial role in coordinating the hydroxyl groups at C6 of the GlcNAc and Gal residues. This bound conformation also demonstrates clearly that only an α(1,3)Gal linkage can be accommodated as the hydroxyl group at C4 of Gal points directly to Tyr[488]. Glycans with α(1,4)Gal linkage would encounter steric hindrance with Tyr[488] and hence do not bind at this αGal/Galili binding site. A similar important role is played by Tyr[492] that holds the terminal Gal unit in place. Molecular docking of the P$_1$ antigen (Fig. 5D) showed that the methyl protons of the *N*-acetamido group of the reducing GlcNAc residue are involved in strong hydrophobic interactions with the Trp[483]. Thr[481], Asp[394], and Ser[396] are all involved in strong hydrophobic interactions coordinating the GlcNAc and Gal residues. The α(1,4)Gal linkage is easily coordinated by this P$_1$ binding site, and no steric hindrances could be observed. In summary, molecular docking studies revealed the most favorable binding affinity for the P$_1$ antigen when bound to the Asp[394]/Ser[396] site and for the αGal/Galili epitope when coordinated by the Arg[465]/Asp[469] site; this corresponds with the signal intensity changes observed in the ^{1}H-^{15}N HSQC NMR data. From these results, we conclude that SLY D4 has two binding sites—one with a high affinity and α(1,3)-Gal specificity (the αGal/Galili binding site) and another with a preference for α(1,4)-Gal linkages (the P$_1$ binding site), as shown in Fig. 5 (C and D). Our experiments also suggest that the P$_1$ binding site has a low affinity for α(1,3)-Gal–containing glycans.

Site-directed mutagenesis was performed in the full-length SLY protein on residues identified in NMR experiments and molecular modeling analyses. Mutagenesis was also performed on Thr[481], which was identified as a key residue for binding to the P$_1$ antigen in the molecular modeling analyses only. The following SLY mutants were
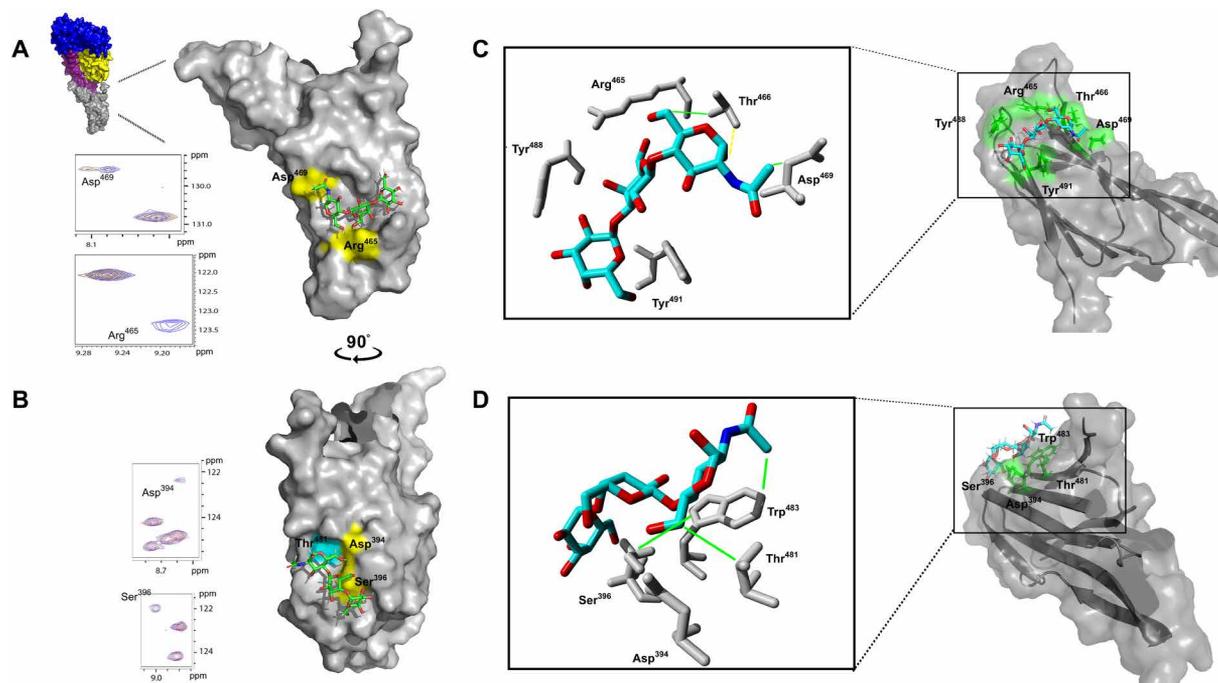
Fig. 5. NMR, molecular dynamics and site-directed mutagenesis, confirmed structures of SLY D4 engaged with two distinct glycan receptors. Sections of ^{1}H-^{15}N HSQC NMR CSP spectra of SLY D4 in the presence of αGal/Galili antigen (**A**) and P$_1$ antigen (**B**) at a protein:ligand ratio of 1:10. Signals of *apo*-SLY D4 are shown in blue and SLY D4 in complex with glycans are shown in red. Full ^{1}H-^{15}N HSQC NMR CSP spectra are shown in fig. S6 (B and C). Amino acids that showed an intensity change or CSP are highlighted in yellow in the SLY D4 structure. Unbiased docking experiments of SLY D4 with αGal/Galili antigen (**C**) and P$_1$ antigen (**D**) represent an energetically favored bound conformation. Both modeled structures are in excellent agreement with ^{1}H-^{15}N HSQC NMR titration experiments (see Fig. 5, A and B). Binding residues identified in molecular docking experiments only are highlighted in cyan. Coordinating amino acids are shaded in green. Dotted yellow bars represent hydrogen bonds. Green bars represent strong hydrophobic interactions, whereas orange bars represent weaker hydrophobic interactions. For an enlarged version of (C) and (D) showing the key coordinating residues, see fig. S6D. See table S3 for SPR analysis of site-directed mutants of key coordinating residues highlighted in (A) and (B). The whole SLY toxin crystal structure is shown in blue (D1), purple (D2), yellow (D3), and gray (D4) in (A) (Protein Data Bank code 3HVN). ppm, parts per million.

analyzed by SPR: R465A, D469A, D394A, S396A, and T481A (table S3). SLY R465A showed an approximately 15-fold reduction in binding to the Galili epitope. Binding to the P$_1$ antigen was not greatly affected, with a slight increase in affinity observed. The SLY D469A mutant also had decreased binding to the Galili epitope (approximately fivefold) and an increase in binding to the P$_1$ antigen (approximately twofold) compared to the wild-type protein. The SLY D394A mutant showed a twofold reduction in binding to the P$_1$ antigen with a similar affinity to wild-type SLY for the Galili epitope, while the SLY S396A mutant showed an approximate fourfold reduction in binding to the P$_1$ antigen with no significant difference in binding to the Galili epitope compared to the wild-type protein. The SLY T481A mutant had an approximate 11-fold reduction in binding to the P$_1$ antigen with no negative impact on binding to the Galili epitope.

The relationship between high-affinity glycan receptors and cholesterol
To investigate the relationship between these newly discovered glycan receptors and cholesterol, we conducted SPR measurements over a range of concentrations of cholesterol, including sub–critical micellar concentrations (CMCs) [25 to 40 nM at 25°C; (*31*)], to provide a like-for-like comparison with glycan receptors using this sensitive label-free biophysical approach. The data shown in Table 1 (also table S1) indicate that Ply, SLO, and LLO have high-affinity interactions with cholesterol, whereas the other CDCs had no detectable concentration-dependent interaction with cholesterol up to 10 µM.

We conducted SPR competition studies between cholesterol and the respective glycan receptors for Ply, SLO, and LLO (table S1 and fig. S7, A to E). These studies demonstrated that there is no competition between the binding of cholesterol and the high-affinity glycan receptors, indicating that the cholesterol and glycans bind to Ply, SLO, and LLO independently.

We screened 3141 drugs, small molecules, and dyes against Ply and SLO by SPR to identify drugs that can block CDC action. In this screen, we discovered that pregnenolone binds to both CDCs (data S2, AC-i and AC-ii). Pregnenolone is a steroid hormone synthesized from cholesterol (fig. S7F) (*32*). Pregnenolone sulfate (PS) is a soluble form of pregnenolone. The K_D of Ply for PS and pregnenolone is not significantly different (both at ~400pM; see table S1). SPR analysis showed that PS binds with high affinity to Ply, SLO, and LLO and with lower affinity to PFO, LLY, and SLY (Table 1 and table S1). Competitive SPR analysis of Ply, SLO, and LLO with cholesterol and PS showed that PS can compete directly with cholesterol, indicating that they bind to the same site on these CDCs. PS could not compete for binding of the high-affinity glycan receptors to Ply, SLO, and LLO, indicating that PS and the glycans bind these CDCs at independent sites (fig. S7).

Investigating the relative contributions of engagement of CDCs with glycan receptors and cholesterol in the initiation of the multistep process of CDC hemolytic activity is difficult to resolve because of the relative insolubility of cholesterol compared to the solubility of glycan receptors. In previous studies, cholesterol has typically

been provided at concentrations higher than the CMC (*5*, *27*, *33*) and often in the form of a liposome or extruded membrane (*34*, *35*), thus differentiating between a CDC binding to cholesterol and the subsequent pore formation steps (oligomerization/prepore, vertical collapse, and transmembrane pore) is difficult. Our observation that PS can act as a soluble cholesterol analog provides an opportunity to test the independent roles of glycans and membrane cholesterol as RBC surface receptors in hemolytic assays. As an exemplar, we used SLO, which has high-affinity interactions with both a glycan (blood group B type IV pentasaccharide, K_D = 116pM) and cholesterol (K_D = 52.3 nM) in hemolytic assays. We showed that the high-affinity glycan receptor, blood group B type IV pentasaccharide, and PS can both inhibit SLO hemolytic activity (fig. S7, I and J). When these molecules are provided in combination, a synergistic inhibitory effect is observed (Fig. 2H). These data further support the idea that the glycan receptor and PS are binding to distinct sites on SLO and also that they are likely blocking sequential steps in SLO-mediated hemolysis.

DISCUSSION

Our findings reveal that lectin activity is a widespread feature of CDCs and is mediated via D4. These data suggest that glycoprotein and/or glycolipid receptors present on the cellular membrane contribute to the cell and tissue tropism of the CDCs. In some cases, the glycan targets that we have identified offer an explanation for the cell tropism of the toxin and thus the pathologies caused by the bacterial species producing the CDC. For example, PLY is known to target human neutrophils and macrophages (*36*), and its glycan target, sLeX, is highly expressed on these cell types (*37*). In another example, the C-series gangliosides are expressed in the human brain during embryonic development (*38*) and are expressed on neural progenitor cells in the adult human brain (*39*). Listeriosis can result in meningitis and has one of the highest mortality rates of any bacterial meningitis (*40*). The potential tropism of LLO for stem cells bearing these receptors, which are required for repairing neuronal damage, may play a role in this disease pathology.

The range of glycans bound by the CDCs varies widely. Ply and LLY only bind to one class of glycan structure, while others, such as PFO, bind to a broad range of glycan structures. Our studies with SLY have shown that D4 of SLY has multiple glycan binding sites, allowing this toxin to accommodate different types of glycan targets. This does not appear to be the case for SLO, which has very broad lectin activity for a related set of galactose-containing structures. Regardless of this broad lectin activity, its highest affinity ligand, blood group B type IV pentasaccharide, with a remarkable K_D of 116 pM (Table 1) can completely block SLO hemolytic activity at the hemolytic dose 100 (HD$_{100}$). These data suggest that SLO may have a single glycan binding site that can no longer interact with any other glycan structures when occupied by its highest affinity ligand.

We demonstrate that Ply uses Mac-1 as a cellular receptor to partly mediate killing of human phagocytic cells and that engagement of Mac-1 is influenced by binding to a sLeX *N*-glycan present on the I-domain of CD11b. These data are supported by the observation that purified Ply can pull down CD11b from a lysate of primary human monocyte-derived dendritic cells, reported in a recent study focusing on the identification of a noncytotoxic cellular receptor for Ply, the mannose receptor C type 1 (*41*). Similarly, we have shown that hCD59 is a compound cellular receptor for ILY, comprising a polypeptide and *O*-linked glycans that have distinct and essential

roles in the efficient engagement of ILY. The potential *O*-glycosylation sites of human erythrocyte CD59 have been identified as Thr[51] and Thr[52] (*28*). In support of our findings, the binding site of a monoclonal antibody that can completely block ILY binding to human RBCs has been mapped to the amino acid residue directly next to the two identified *O*-glycosylation sites of hCD59 (Arg[53]) (*7*). Note that the residues of hCD59 to which ILY binds are amino acids 42 to 58 (*7*), encompassing the *O*-glycosylation sites.

While it is accepted that the CDCs interact with membrane cholesterol to form functional pores, cholesterol acting as the sole cellular receptor for these toxins does not fully explain cellular tropism. For example, mouse RBCs are far more resistant to SLO hemolytic activity than human and rabbit RBCs, despite RBCs from these species having similar cholesterol content (*42*). For ILY, which does not use cholesterol as a receptor (*9*), the proposed role of cholesterol in pore formation is to anchor the oligomerized toxin to the membrane surface as it disengages from hCD59 during prepore to transmembrane pore conversion (*6*, *43*, *44*). Here, we demonstrate that the hCD59 interaction involves ILY lectin activity. On the basis of our data, showing independent binding of glycans and cholesterol by Ply, SLO, and LLO, we propose that the role of glycoconjugate receptors in CDC pore formation is as follows: There is an initial interaction of the soluble CDC monomer via D4 with a glycan receptor on the cell surface, directing and accumulating the toxin monomer to its target cell, followed by disengagement from the glycan receptor, and lastly an interaction with the membrane during the transition from the prepore to the transmembrane pore. This proposed role for glycan receptors as an initial point of contact for the toxin to host cells before the pore-formation process is further supported by the synergistic inhibitory effect we observed with the exogenous cholesterol analog, PS, and exogenous glycan receptor in blocking SLO hemolytic activity, suggesting that two crucial, independent steps are being inhibited. These data are consistent with the model for CD59 as the receptor for ILY described in previous work by others (*6*, *43*, *44*). In addition to this newly defined role for glycoconjugate receptors in directing CDCs to particular target cells as the first step in the pore formation process, these receptors may also play an important role in the tropism of the well-described sublytic effects of CDCs on host cells (*45*).

We report a wide spectrum of binding affinities between CDCs and cholesterol. Ply, SLO, and LLO have high-affinity interactions. PFO, LLY, and SLY have no detectable interactions with cholesterol but did recognize the soluble cholesterol analog, PS, presumably due to its greater solubility at higher concentrations. Moreover, consistent with other reports (*7*), we observe that ILY binds neither cholesterol nor PS. Regardless of the lack of a direct high-affinity interaction between the CDCs and cholesterol, this sterol is important for pore formation for all CDCs, perhaps by imparting biophysical properties to the membrane that are highly conducive to the latter steps in the multistep, pore-formation process. Note that all of the glycan receptors identified in this study typically exist as glycoproteins, glycolipids, and GPI-anchored glycoproteins that are frequently associated with the periphery of cholesterol-rich lipid rafts. The classic reagent used to define the periphery of a lipid raft is cholera toxin, which targets the glycolipid GM1 (Ganglioside-monosialic acid 1) (*46*). Therefore, the identification of glycan receptors for all major CDCs and their role in initial cell contact, thereby imparting cell and tissue tropism, is consistent with a subsequent interaction of the CDCs with a cholesterol-rich lipid raft that is immediately adjacent to these glycoconjugate

receptors on the cell surface. We have confirmed the importance and relevance of these receptors in toxin function using the ex vivo human model system of hemolytic activity assays, which is a common and well-accepted assay for this entire class of toxins. The identification of these glycan receptors for each of the CDCs studied here opens the door to further detailed analysis of the role of these glycans in cell, tissue, and host specificity. We anticipate that, like the example of ILY where we have shown that glycans are a crucial component of the CD59 cellular receptor, the glycoproteins and glycolipids that carry the glycan receptors for other CDCs identified here will be discovered, which will help to explain toxin tropism. The identification of these receptors and the molecular mechanisms of their engagement by D4 of the CDCs, exemplified by SLY, will facilitate studies on small-molecule inhibitors and precisely targeted immunological strategies for prevention and treatment of diseases caused by this important group of human pathogens.

MATERIALS AND METHODS
Cloning, expression, and purification of CDCs, domains, and mutants

Ply and SLO were expressed and purified as previously described (9). PFO, LLY, and LLY without the lectin domain, VLY, and ILY were expressed and purified as previously described (47–49). Primers were designed to amplify sequences encoding the following: LLO without the signal sequence (residues 25 to 529) and D4 of LLO (residues 415 to 529) from *L. monocytogenes* American Type Culture Collection 9525, SLY without the signal sequence (residues 28 to 497) and D4 of SLY (residues 389 to 497) from *S. suis* strain P1/7, and D4 of ILY (residues 416 to 532) (accession no. AB029317.1). DNA used as template in polymerase chain reactions (PCRs) was purchased from Integrated DNA Technologies. Amplified sequences were cloned into the expression vector pET-15b (Novagen) and were confirmed by DNA sequencing. SLY site-directed mutants were created using inverse PCR to introduce mutations into the sly_pET-15b expression construct. The resultant His-tagged expression constructs were transformed into *Escherichia coli* BL21 (DE3) for protein expression. Bacterial cultures were grown in Luria-Bertani broth/Amp at 30°C with 200 rpm shaking until an optical density at 600 nm (OD_{600}) of ~0.4 was reached. Protein expression was induced with 0.5 mM isopropyl-β-D-thiogalactopyranoside (IPTG) final concentration for 20 hours at 30°C or for 16 hours at 37°C for SLY and SLY D4. Cells were harvested, resuspended in a wash buffer [50 mM sodium phosphate and 300 mM NaCl (pH 7.0)] with deoxyribonuclease (10 μg/ml), lysozyme (1 mg/ml), and EDTA-free protease inhibitor cocktail (Roche). Cells were freeze/thawed and then lysed further with 0.1-mm glass beads using a Qiagen TissueLyser. Soluble His-tagged proteins were purified using TALON cobalt metal affinity resin (Takara Bio) according to the manufacturer's protocol. Protein concentration was determined using a BCA (Bicinchoninic Acid) protein assay kit (Thermo Fisher Scientific). SDS–polyacrylamide gel electrophoresis (PAGE) analysis of purified recombinant CDCs is shown in fig. S1.

Glycan array

Glycan array slides were printed on SuperEpoxy 3–activated substrates as previously described (50) using the list of glycans previously described in (51) with the addition of glycan IDs 17A to 19P to the glycan library (also see data S1). Glycan array slides were blocked

with 0.1% bovine serum albumin (BSA) in phosphate-buffered saline (PBS) with 2 mM $MgCl_2/CaCl_2$ (assay PBS) for 5 min. One microgram of His-tagged Ply, SLO, PFO, LLY, VLY, LLO, SLY, and ILY was diluted to 400 μl in assay PBS with precomplexed anti-His monoclonal antibody (Sigma-Aldrich), rabbit anti-mouse Alexa Fluor 555 (Life Technologies), and goat anti-rabbit Alexa Fluor 555 antibodies (Life Technologies) and bound to the glycan array for 15 min at room temperature. Slides were washed twice for 5 min in assay PBS to remove excess protein and were then fixed with 5% formaldehyde in PBS. The slides were lastly dried by centrifugation in a 50-ml tube for 5 min at 150g. The array slides were scanned with a ProScan Array scanner at 555/565 nm, and the results were analyzed using ScanArray Express software (PerkinElmer). Background relative fluorescence units (RFU) was defined as the average fluorescence of 12 sets of blank spots plus 3SDs of the mean. Binding was therefore defined as visible spots with an RFU value greater than 1 when average fluorescence of printed glycan spots was divided by background RFU (blank spot mean + 3SD). Statistical analysis of the data was performed by a Student's *t* test with a confidence level of 99.99% ($P \leq 0.0001$).

SPR analysis

SPR is a label-free method for testing interactions between two molecules. Using the Biacore T200 system used in these experiments, a minimum of two response units (RU) at the highest concentration tested is required for valid analysis. No data presented in this publication were determined from responses lower than 5 RU at the highest concentration tested. Interactions between the CDC proteins/domains and test glycans were analyzed using SPR as described by Shewell *et al.* (9), with the following modifications. Proteins were immobilized onto a CM5 chip at pH 4.5 with a flow rate of 5 μl/min for 600 s with an ethanolamine blank flow cell (FC) as a control. The CDCs were captured three at a time on FC2, FC3, and FC4, and due to this arrangement, data obtained from FC3 and FC4 contained timing spikes caused by the double reference subtraction with the data from FC3 and FC4, in particular, being out of phase with the data on FC1. This does not affect the analysis of the data as the region of the curves containing these spikes is not used for calculation of the affinity of the interactions. The range of CDC levels captured on CM5 sensor chips varies for each protein sample. Because of capture level differences between proteins and experiments, no direct RU comparison between tested glycans can be performed with the raw sensorgrams displayed in data S2. Glycans were initially tested between 160 nM and 100 μM, with 1:5 dilutions. Final concentrations of glycans were adjusted based on where saturation was observed, with 100 μM being the maximum concentration used. Representative sensograms from triplicate repeat experiments are shown in data S2. All glycans were obtained from Elicityl (France), except for cellobiose, which was obtained from Carbosynth (UK). All glycans were analyzed by NMR and high performance anion exchange chromatography for structure validation and purity by the supplier. sLeC (Neu5Acα2-3Galβ1-3GlcNAc), sTF (Neu5Acα2-3Galβ1-3GalNAc), and TF (Galβ1-3GalNAc) were synthesized as previously described (52). Cholesterol was sourced from Sigma-Aldrich, and PS (sodium salt; soluble up to 500 μM in aqueous buffers) was sourced from Steraloids Inc. (Newport, RI., USA). Cholesterol was tested at a range of concentrations (1.6 nM to 10 μM), which represents a range of physical states from soluble monomeric (<25 to 40 nM), to rod-like micelles (>25 to 40 nM) (53), to insoluble complexes (>5 μM). SPR

studies with Mac-1 (R&D Systems) and recombinant I-domain were conducted as previously described (*24*). The presence of a *N*-linked sLeX glycosylation in the I-domain of the recombinant Mac-1 produced in Chinese hamster ovary cells (R&D Systems) was confirmed by NanoLC–tandem mass spectrometry (MS/MS) analysis (see below). Removal of *N*-linked sLeX from Mac-1 was achieved by incubation with peptide *N*-glycosidase F (PNGase F) (New England Biolabs) and confirmed by SPR analysis with anti-sLeX monoclonal antibody (clone 258-12767, Creative Diagnostics).

NanoLC-MS/MS analysis
Recombinant Mac-1 (R&D Systems) was analyzed by reverse-phase high-performance liquid chromatography–electrospray ionization–tandem mass spectrometry (HPLC-ESI-MS/MS) using a Dionex UltiMate 3000 RSLC nano-LC system (Thermo Fisher Scientific) connected to an Orbitrap Fusion Tribrid mass spectrometer (Thermo Scientific) with details described in the Supplementary Materials.

Cytotoxicity assays
Hemolytic assays were performed essentially as previously described (*9*), with the following modifications: CDCs were prereduced at a concentration of 100 μg/ml with 2 mM dithiothreitol, except for ILY; absorbance of released hemoglobin was measured at 417 nm. Human RBCs were provided by the Australian Red Cross under material supply agreement 17-02QLD-18.

Cytotoxicity assays against THP-1 cells were performed as previously described (*24*), except rather than intoxication with a purified toxin, a multiplicity of infection of 2.5 of *S. pneumoniae* D39 were added to the cells. A nontoxic Ply mutant was used to demonstrate that the cytotoxic effect observed was Ply dependent. shRNA knockdown of CD11b expression (*26*) was used to demonstrate that Ply cytotoxicity was CD11b dependent.

Inhibition of CDC hemolytic activity with candidate glycan receptors
The minimum concentration of toxin able to achieve approximately 100% lysis of 1% (v/v) human group O RBCs (HD_{100}) was determined for each CDC by titrating the toxin against the particular donor RBCs before performing inhibition of hemolytic activity assays (see fig. S8 for examples). CDCs at the HD_{100} were preincubated with the appropriate concentration of exogenous free glycan in PBS for 15 min at room temperature before the addition of a final concentration of 1% (v/v) of human group O RBCs. Cellobiose was used in all assays as a nonbinding glycan control. For analysis of the combination of blood group B type IV pentasaccharide and PS against SLO (Fig. 2H), SLO at the HD_{100} (fig. S7G) was preincubated with the indicated concentration of free glycan, PS (sodium salt), or a combination of free glycan and PS before the addition of 1% (v/v) of human group O RBCs. In cases of CDCs with multiple candidate glycan receptors (PFO and SLY), where the blocking effect of a single glycan may be masked by the presence of multiple distinct receptors, HD_{50} was used in inhibition assays to increase sensitivity. It was observed during hemolytic assays that particular glycans (sTF and Neu5Acα2-6LacNAc) caused agglutination or aggregation of RBCs, resulting in a nonspecific protective effect against hemolysis. There are previous reports of carbohydrates in the form of polysaccharides causing hemagglutination (*54*). In the case of ILY, where this agglutination or aggregation was observed, whole RBC enzyme-linked immunosorbent assay (ELISA) was used to assess binding of toxin to the RBC surface (see the method below). Several CDCs recognize receptors terminating with sialic acid. An obvious strategy, in addition to inhibiting hemolytic activity with exogenous free glycan, described above, is to treat the cells with neuraminidase to remove the candidate sialylated receptor. Whole RBCs could not be treated with neuraminidase as this caused aggregation of the RBCs and interfered with hemolytic activity assays, presumably due to the reduction in net surface charge (*55*).

Analysis of RBC surface binding by flow cytometry
Flow cytometry analyses were performed essentially as previously described (*9*), with modifications and details described in the Supplementary Materials.

Whole RBC ELISA
Whole RBC ELISA was performed as described by Koganei *et al.* (*56*), with minor modifications and details described in the Supplementary Materials.

Biotin labeling of ILY
ILY was labeled with biotin using the EZ-link Micro Sulfo-NHS-Biotinylation Kit (Thermo Fisher Scientific) as per the manufacturer's instructions using a fivefold molar excess of biotin reagent. The hemolytic activity of ILY following labeling was examined in a hemolytic assay and was found to be no different from unlabeled ILY.

Far Western/Western blot analyses
Solubilized RBC membrane proteins (described in the Supplementary Materials) were prepared by incubating 100 μg of RBC membranes with a final concentration of 3% (w/v) of 3-[(3-cholamidopropyl) di-methylammonio]-1-propanesulfonate in a 20 μl of reaction volume for 60 min at room temperature. Soluble and insoluble fractions were separated by centrifugation at 13,000*g* for 60 min at room temperature. Soluble RBC membrane proteins were treated with enzyme buffer only, α2-3 neuraminidase, both α2-3 neuraminidase and *O*-glycosidase or PNGase. The *O*-glycosidase used removes core 1 (Galβ1-3GalNAc) and core 3 (GlcNAcβ1-3GalNAc) *O*-linked disaccharides from glycoproteins. Sialic acid residues must be removed to allow this *O*-glycosidase to cleave *O*-linked glycans. All enzymes were from New England Biolabs and used as recommended by the manufacturer's instructions. Untreated and treated soluble RBC membrane proteins were combined with LDS (lithium dodecyl sulfate) sample buffer without reducing agent and boiled for 10 min. Proteins were separated on a NuPAGE 4 to 12% bis-tris gel (Life Technologies) with NuPAGE MES SDS running buffer (Life Technologies) and then transferred to a nitrocellulose membrane. Membranes were blocked with 5% BSA in PBS for 60 min at room temperature. Equal loading of protein samples was confirmed by staining with Coomassie blue. hCD59 was detected using a CD59-purified MaxPab mouse polyclonal antibody (Abnova) at 1:1000 as primary antibody and anti-mouse immunoglobulin horseradish peroxidase antibody (Dako) at 1:10,000 as secondary antibody for 60 min at room temperature. For far-Western analyses, the membrane containing transferred solubilized RBC membrane proteins was incubated with ILY-biotin (500 ng/ml) for 2 hours at room temperature, washed three times for 5 min with PBS, incubated with streptavidin-peroxidase (Sigma-Aldrich) at 1:10,000 for 60 min at room temperature, and then washed three times for 5 min with PBS. Blots were developed by the addition of SuperSignal West Pico Chemiluminescence Substrate (Thermo Fisher Scientific) as per the manufacturer's instructions.

Expression of double-labeled (^{13}C-^{15}N) SLY D4

Double-labeled ^{13}C and ^{15}N SLY D4 was produced by growing *E. coli* strain BL21 (DE3) transformed with the SLY D4 expression construct (slyD4_pET15b) in M9 minimal media containing N_{15} NH_4Cl (1 g/liter) as a nitrogen source and C_{13} glucose (4 g/liter) as a carbon source. Cells were grown to mid-log phase (OD_{600} of ~0.35), induced with 0.5 mM IPTG final concentration, and then grown overnight at 37°C with 200 rpm shaking. SLY D4 containing a N-terminal 6xHis tag was purified using TALON cobalt metal affinity resin (Takara Bio) according to the manufacturer's protocol with further details provided in the Supplementary Materials.

NMR spectroscopy

Uniformly ^{13}C- and ^{15}N-labeled purified SLY D4 was dissolved in 180 µl of 10 mM phosphate buffer (pH 7.4) containing 50 mM NaCl and 2.7 mM KCl in 10% D_2O, and 90% H_2O to a final concentration of 0.5 mM SLY D4. 4,4-dimethyl-4-silapentane-1-sulfonic acid (DSS) was added as internal calibration standard. NMR experiments were carried out at 298 K (25°C) on a 600-MHz Bruker Avance spectrometer fitted with a 5-mm triple resonance cryoprobe, and a 600-MHz Agilent DD2 NMR spectrometer was also equipped with a cold probe (Creative Biostructures, NY, USA). ^{1}H NMR, 2D ^{1}H-^{15}N HSQC, 3D HNCACB, and 3D CBCA(CO)NNH experiments were acquired. Proton chemical shifts were referenced against external DSS, whereas nitrogen chemical shifts were referenced indirectly to DSS using the absolute frequency ratio. One hundred twenty-eight data points in the t_1 domain and 1024 data points in the t_2 dimension were collected. The sweep width was 18.0 parts per million (ppm) in the ^{1}H dimension and 31.8 ppm in the ^{15}N dimension. Triple resonance (^{1}H/^{13}C/^{15}N) NMR experiments were recorded with 128 increments in the t_1 domain, 40 increments in the t_2 domain, and 2048 increments in the t_3 domain. Spectra were processed using TopSpin and VnmrJ and analyzed using NMRPipe and CCPNmr. Secondary structure assignments were generated by the backbone chemical shift analysis program DANGLE incorporated in the CCPNmr software.

Backbone assignment of uniformly labeled ^{13}C-^{15}N SLY D4

Backbone ^{1}H$_N$, ^{15}N, ^{13}Cα, and ^{13}Cβ chemical shifts were assigned for SLY D4 using standard triple resonance methodology, with details provided in the Supplementary Materials.

^{1}H-^{15}N HSQC titration experiments of SLY D4 in complex with Galili and P_1 antigen

^{15}N HSQC experiments were acquired using a phosphate buffer (pH 7.4) containing 50 mM NaCl and 2.7 mM KCl in 10% D_2O and 90% H_2O to a final concentration of 0.05 mM SLY D4 in 200 µl of total volume. Galili epitope was added at a protein:ligand ratio of 1:0.1, 1:0.5, 1:1, 1:5, and 1:10, whereas P_1 antigen was added resulting in protein:ligand ratios of 1:1, 1:2, and 1:10. Cellobiose was added at a protein:ligand ratio of 1:10 to serve as a nonbinding glycan control. All ^{1}H-^{15}N HSQC titration experiments NMR were carried out at 298 K (25°C) on a 600-MHz Bruker Avance spectrometer fitted with a 5-mm triple resonance cryoprobe equipped with a cold probe. Data points in F2 were set to 256 with a total number of scans of 16.

Molecular modeling

To evaluate a potential binding site of the P_1 and Galili antigens, a docking experiment was performed using the AutoDock Vina pro-

tocol (*57*). It has been shown that AutoDock Vina has the highest scoring power among commercial and academic molecular docking programs (*58*) implemented in the YASARA molecular modeling package (ver. 16.46) (*59*).

An unbiased global docking experiment of α-galactose was conducted with a box size of 40 × 40 × 40 Å (Trp^{436}), covering two-thirds of the protein surface. Results from these docking experiments revealed two frequently occupied ligand sites. These sites were used for a local docking experiment of the Galili and P_1 antigen. The preferred Galili epitope binding site was found close to Arg^{465}, which showed significant intensity changes in the ^{1}H-^{15}N HSQC NMR experiments. Docking results from the P_1 antigen resulted in a low-energy conformation at a site involving Ser^{396} that also is in excellent agreement with the ^{1}H-^{15}N HSQC NMR results. Our unbiased NMR and molecular modeling approach has revealed two independent major glycan binding sites with distinct linkage specificity.

Drug library screening of Ply and SLO

Ply and SLO were immobilized to a CM5 sensor chip as described above. A combination of two drug libraries, Microsource-CPOZ (2400 drugs) and ML Drug (741 drugs), comprising U.S. Food and Drug Administration–approved drugs and other small-molecule compounds were purchased from Compounds Australia and binding screened by SPR analysis. The analysis was performed as previously described (*60*).

Data availability statement

The ^{1}H$_N$, ^{15}N, ^{13}Cα, and ^{13}Cβ spectra for SLY D4 were deposited in the BioMagResBank (BMRB) (www.bmrb.wisc.edu/) under the BMRB accession code 27707. All other data generated or analyzed during this study are included in this manuscript and in the Supplementary Materials.

Statistical analysis

Data were analyzed for statistical significance with Prism 5 software (GraphPad Software Inc.) using a two-tailed unpaired Student's t test. $P < 0.05$ was considered significant.

SUPPLEMENTARY MATERIALS

Supplementary material for this article is available at http://advances.sciencemag.org/cgi/content/full/6/21/eaaz4926/DC1

View/request a protocol for this paper from *Bio-protocol*.

REFERENCES AND NOTES

1. O. Shatursky, A. P. Heuck, L. A. Shepard, J. Rossjohn, M. W. Parker, A. E. Johnson, R. K. Tweten, The mechanism of membrane insertion for a cholesterol-dependent cytolysin: A novel paradigm for pore-forming toxins. *Cell* **99**, 293–299 (1999).

2. C. Leung, N. V. Dudkina, N. Lukoyanova, A. W. Hodel, I. Farabella, A. P. Pandurangan, N. Jahan, M. P. Damaso, D. Osmanović, C. F. Reboul, M. A. Dunstone, P. W. Andrew, R. Lonnen, M. Topf, H. R. Saibil, B. W. Hoogenboom, Stepwise visualization of membrane pore formation by suilysin, a bacterial cholesterol-dependent cytolysin. *eLife* **3**, e04247 (2014).

3. L. F. Hewitt, E. W. Todd, The effect of cholesterol and of sera contaminated with bacteria on the haemolysins produced by haemolytic streptococci. *J. Pathol. Bacteriol.* **49**, 45–51 (1939).

4. T. Nishibori, H. Xiong, I. Kawamura, M. Arakawa, M. Mitsuyama, Induction of cytokine gene expression by listeriolysin O and roles of macrophages and NK cells. *Infect. Immun.* **64**, 3188–3195 (1996).

5. T. Jacobs, A. Darji, N. Frahm, M. Rohde, J. Wehland, T. Chakraborty, S. Weiss, Listeriolysin O: Cholesterol inhibits cytolysis but not binding to cellular membranes. *Mol. Microbiol.* **28**, 1081–1098 (1998).

6. C. M. Boyd, E. S. Parsons, R. A. G. Smith, J. M. Seddon, O. Ces, D. Bubeck, Disentangling the roles of cholesterol and CD59 in intermedilysin pore formation. *Sci. Rep.* **6**, 38446 (2016).

7. K. S. Giddings, J. Zhao, P. J. Sims, R. K. Tweten, Human CD59 is a receptor for the cholesterol-dependent cytolysin intermedilysin. *Nat. Struct. Mol. Biol.* **11**, 1173–1178 (2004).

8. A. L. DuMont, V. J. Torres, Cell targeting by the Staphylococcus aureus pore-forming toxins: it's not just about lipids. *Trends Microbiol.* **22**, 21–27 (2014).

9. L. K. Shewell, R. M. Harvey, M. A. Higgins, C. J. Day, L. E. Hartley-Tassell, A. Y. Chen, C. M. Gillen, D. B. James, F. Alonzo III, V. J. Torres, M. J. Walker, A. W. Paton, J. C. Paton, M. P. Jennings, The cholesterol-dependent cytolysins pneumolysin and streptolysin O require binding to red blood cell glycans for hemolytic activity. *Proc. Natl. Acad. Sci. U.S.A.* **111**, E5312–E5312 (2014).

10. J. Rossjohn, S. C. Feil, W. J. McKinstry, R. K. Tweten, M. W. Parker, Structure of a cholesterol-binding, thiol-activated cytolysin and a model of its membrane form. *Cell* **89**, 685–692 (1997).

11. T. C. Barnett, J. N. Cole, T. Rivera-Hernandez, A. Henningham, J. C. Paton, V. Nizet, M. J. Walker, Streptococcal toxins: Role in pathogenesis and disease. *Cell. Microbiol.* **17**, 1721–1741 (2015).

12. M. Jeyakanthan, K. Tao, L. Zou, P. J. Meloncelli, T. L. Lowary, K. Suzuki, D. Boland, I. Larsen, M. Burch, N. Shaw, K. Beddows, L. Addonizio, W. Zuckerman, B. Afzali, D. H. Kim, M. Mengel, A. M. Shapiro, L. J. West, Chemical basis for qualitative and quantitative differences between ABO blood groups and subgroups: Implications for organ transplantation. *Am. J. Transplantation* **15**, 2602–2615 (2015).

13. D. L. Stevens, A. E. Bryant, The role of clostridial toxins in the pathogenesis of gas gangrene. *Clin. Infect. Dis.* **35**, S93–S100 (2002).

14. D. K. O'Brien, S. B. Melville, Effects of Clostridium perfringens alpha-toxin (PLC) and perfringolysin O (PFO) on cytotoxicity to macrophages, on escape from the phagosomes of macrophages, and on persistence of C. perfringens in host tissues. *Infect. Immun.* **72**, 5204–5215 (2004).

15. M. Pleckaityte, M. Janulaitiene, R. Lasickiene, A. Zvirbliene, Genetic and biochemical diversity of Gardnerella vaginalis strains isolated from women with bacterial vaginosis. *FEMS Immunol. Med. Microbiol.* **65**, 69–77 (2012).

16. H. Ohkuni, H. Nagamune, N. Ozaki, A. Tabata, Y. Todome, Y. Watanabe, H. Takahashi, K. Ohkura, H. Kourai, H. Ohtsuka, V. A. Fischetti, J. B. Zabriskie, Characterization of recombinant Streptococcus mitis-derived human platelet aggregation factor. *Acta Pathol. Microbiol. Immunol. Scand.* **120**, 56–71 (2012).

17. S. Farrand, E. Hotze, P. Friese, S. K. Hollingshead, D. F. Smith, R. D. Cummings, G. L. Dale, R. K. Tweten, Characterization of a streptococcal cholesterol-dependent cytolysin with a lewis y and b specific lectin domain. *Biochemistry* **47**, 7097–7107 (2008).

18. A. Tabata, K. Ohkura, Y. Ohkubo, T. Tomoyasu, H. Ohkuni, R. A. Whiley, H. Nagamune, The diversity of receptor recognition in cholesterol-dependent cytolysins. *Microbiol. Immunol.* **58**, 155–171 (2014).

19. B. N. Nguyen, B. N. Peterson, D. A. Portnoy, Listeriolysin O: A phagosome-specific cytolysin revisited. *Cell. Microbiol.* , e12988 (2018).

20. C. Geoffroy, J. L. Gaillard, J. E. Alouf, P. Berche, Purification, characterization, and toxicity of the sulfhydryl-activated hemolysin listeriolysin O from Listeria monocytogenes. *Infect. Immun.* **55**, 1641–1646 (1987).

21. Z. He, Y. Pian, Z. Ren, L. Bi, Y. Yuan, Y. Zheng, Y. Jiang, F. Wang, Increased production of suilysin contributes to invasive infection of the Streptococcus suis strain 05ZYH33. *Mol. Med. Rep.* **10**, 2819–2826 (2014).

22. U. Galili, Interaction of the natural anti-Gal antibody with alpha-galactosyl epitopes: A major obstacle for xenotransplantation in humans. *Immunol. Today* **14**, 480–482 (1993).

23. S. A. Park, Y. S. Park, S. M. Bong, K. S. Lee, Structure-based functional studies for the cellular recognition and cytolytic mechanism of pneumolysin from Streptococcus pneumoniae. *J. Struct. Biol.* **193**, 132–140 (2016).

24. A. L. DuMont, P. Yoong, C. J. Day, F. Alonzo III, W. H. McDonald, M. P. Jennings, V. J. Torres, Staphylococcus aureus LukAB cytotoxin kills human neutrophils by targeting the CD11b subunit of the integrin Mac-1. *Proc. Natl. Acad. Sci. U.S.A.* **110**, 10794–10799 (2013).

25. K. Zen, L. B. Cui, C. Y. Zhang, Y. Liu, Critical role of mac-1 sialyl lewis x moieties in regulating neutrophil degranulation and transmigration. *J. Mol. Biol.* **374**, 54–63 (2007).

26. J. H. Melehani, D. B. James, A. L. DuMont, V. J. Torres, J. A. Duncan, Staphylococcus aureus Leukocidin A/B (LukAB) Kills Human Monocytes via Host NLRP3 and ASC when Extracellular, but Not Intracellular. *PLOS Pathog.* **11**, e1004970 (2015).

27. H. Nagamune, C. Ohnishi, A. Katsuura, K. Fushitani, R. A. Whiley, A. Tsuji, Y. Matsuda, Intermedilysin, a novel cytotoxin specific for human cells secreted by Streptococcus intermedius UNS46 isolated from a human liver abscess. *Infect. Immun.* **64**, 3093–3100 (1996).

28. P. M. Rudd, B. P. Morgan, M. R. Wormald, D. J. Harvey, C. W. van den Berg, S. J. Davis, M. A. Ferguson, R. A. Dwek, The glycosylation of the complement regulatory protein, human erythrocyte CD59. *J. Biol. Chem.* **272**, 7229–7244 (1997).

29. M. P. Christie, B. A. Johnstone, R. K. Tweten, M. W. Parker, C. J. Morton, Cholesterol-dependent cytolysins: From water-soluble state to membrane pore. *Biophys. Rev.* **10**, 1337–1348 (2018).

30. M. P. Williamson, Using chemical shift perturbation to characterise ligand binding. *Prog. Nucl. Magn. Reson. Spectrosc.* **73**, 1–16 (2013).

31. M. E. Haberland, J. A. Reynolds, Self-association of cholesterol in aqueous solution. *Proc. Natl. Acad. Sci. U.S.A.* **70**, 2313–2316 (1973).

32. A. H. Payne, D. B. Hales, Overview of steroidogenic enzymes in the pathway from cholesterol to active steroid hormones. *Endocr. Rev.* **25**, 947–970 (2004).

33. A. F. Sonnen, A. J. Rowe, P. W. Andrew, R. J. Gilbert, Oligomerisation of pneumolysin on cholesterol crystals: Similarities to the behaviour of polyene antibiotics. *Toxicon* **51**, 1554–1559 (2008).

34. S. Shany, A. W. Bernheimer, P. S. Grushoff, K. S. Kim, Evidence for membrane cholesterol as the common binding site for cereolysin, streptolysin O and saponin. *Mol. Cell. Biochem.* **3**, 179–186 (1974).

35. S. Cauci, R. Monte, M. Ropele, C. Missero, T. Not, F. Quadrifoglio, G. Menestrina, Pore-forming and haemolytic properties of the Gardnerella vaginalis cytolysin. *Mol. Microbiol.* **9**, 1143–1155 (1993).

36. H. M. Marriott, T. J. Mitchell, D. H. Dockrell, Pneumolysin: a double-edged sword during the host-pathogen interaction. *Curr. Mol. Med.* **8**, 497–509 (2008).

37. J. M. Munro, S. K. Lo, C. Corless, M. J. Robertson, N. C. Lee, R. L. Barnhill, D. S. Weinberg, M. P. Bevilacqua, Expression of sialyl-Lewis X, an E-selectin ligand, in inflammation, immune processes, and lymphoid tissues. *Am. J. Pathol.* **141**, 1397–1408 (1992).

38. K. Letinic, M. Heffer-Lauc, H. Rosner, I. Kostovic, C-pathway polysialogangliosides are transiently expressed in the human cerebrum during fetal development. *Neuroscience* **86**, 1–5 (1998).

39. M. C. Nunes, N. S. Roy, H. M. Keyoung, R. R. Goodman, G. McKhann II, L. Jiang, J. Kang, M. Nedergaard, S. A. Goldman, Identification and isolation of multipotential neural progenitor cells from the subcortical white matter of the adult human brain. *Nat. Med.* **9**, 439–447 (2003).

40. J. Y. Engelen-Lee, M. M. Koopmans, M. C. Brouwer, E. Aronica, D. van de Beek, Histopathology of Listeria Meningitis. *J. Neuropathol. Exp. Neurol.* **77**, 950–957 (2018).

41. K. Subramanian, D. R. Neill, H. A. Malak, L. Spelmink, S. Khandaker, G. D. L. Marchiori, E. Dearing, A. Kirby, M. Yang, A. Achour, J. Nilvebrant, P.-Å. Nygren, L. Plant, A. Kadioglu, B. Henriques-Normark, Pneumolysin binds to the mannose receptor C type 1 (MRC-1) leading to anti-inflammatory responses and enhanced pneumococcal survival. *Nat. Microbiol.* **4**, 62–70 (2019).

42. J. G. Howard, K. R. Wallace, The comparative resistances of the red cells of various species to haemolysis by streptolysin O and by saponin. *Br. J. Exp. Pathol.* **34**, 181–184 (1953).

43. S. LaChapelle, R. K. Tweten, E. M. Hotze, Intermedilysin-receptor interactions during assembly of the pore complex: assembly intermediates increase host cell susceptibility to complement-mediated lysis. *J. Biol. Chem.* **284**, 12719–12726 (2009).

44. A. J. Farrand, S. LaChapelle, E. M. Hotze, A. E. Johnson, R. K. Tweten, Only two amino acids are essential for cytolytic toxin recognition of cholesterol at the membrane surface. *Proc. Natl. Acad. Sci. U.S.A.* **107**, 4341–4346 (2010).

45. S. K. Cassidy, M. X. O'Riordan, More than a pore: the cellular response to cholesterol-dependent cytolysins. *Toxins* **5**, 618–636 (2013).

46. N. Gupta, A. L. DeFranco, Visualizing lipid raft dynamics and early signaling events during antigen receptor-mediated B-lymphocyte activation. *Mol. Biol. Cell* **14**, 432–444 (2003).

47. S. L. Lawrence, M. A. Gorman, S. C. Feil, T. D. Mulhern, M. J. Kuiper, A. J. Ratner, R. K. Tweten, C. J. Morton, M. W. Parker, Structural basis for receptor recognition by the human CD59-responsive cholesterol-dependent cytolysins. *Structure* **24**, 1488–1498 (2016).

48. S. C. Feil, S. Lawrence, T. D. Mulhern, J. K. Holien, E. M. Hotze, S. Farrand, R. K. Tweten, M. W. Parker, Structure of the lectin regulatory domain of the cholesterol-dependent cytolysin lectinolysin reveals the basis for its lewis antigen specificity. *Structure* **20**, 248–258 (2012).

49. S. C. Feil, J. Rossjohn, K. Rohde, R. K. Tweten, M. W. Parker, Crystallization and preliminary X-ray analysis of a thiol-activated cytolysin. *FEBS Lett.* **397**, 290–292 (1996).

50. C. J. Day, J. Tiralongo, R. D. Hartnell, C.-A. Logue, J. C. Wilson, V. von Itzstein, V. Korolik, Differential carbohydrate recognition by Campylobacter jejuni strain 11168: Influences of temperature and growth conditions. *PLOS ONE* **4**, e4927 (2009).

51. M. Waespy, T. T. Gbem, L. Elenschneider, A. P. Jeck, C. J. Day, L. Hartley-Tassell, N. Bovin, J. Tiralongo, T. Haselhorst, S. Kelm, Carbohydrate Recognition Specificity of Trans-sialidase Lectin Domain from Trypanosoma congolense. *PLoS Negl. Trop. Dis.* **9**, e0004120 (2015).

52. K. Lau, H. Yu, V. Thon, Z. Khedri, M. E. Leon, B. K. Tran, X. Chen, Sequential two-step multienzyme synthesis of tumor-associated sialyl T-antigens and derivatives. *Org. Biomol. Chem.* **9**, 2784–2789 (2011).

53. M. A. Castanho, W. Brown, M. J. Prieto, Rod-like cholesterol micelles in aqueous solution studied using polarized and depolarized dynamic light scattering. *Biophys. J.* **63**, 1455–1461 (1992).

54. X. Zhou, X. Zhang, J. Zhou, L. Li, An investigation of chitosan and its derivatives on red blood cell agglutination. *RSC Adv.* **7**, 12247–12254 (2017).

55. K. M. Jan, S. Chien, Role of surface electric charge in red blood cell interactions. *J. Gen. Physiol.* **61**, 638–654 (1973).

56. A. Koganei, T. Tsuchiya, K. Samura, M. Nishikibe, Use of whole sheep red blood cells in ELISA to assess immunosuppression in vivo. *J. Immunotoxicol.* **4**, 77–82 (2007).

57. O. Trott, A. J. Olson, AutoDock Vina: improving the speed and accuracy of docking with a new scoring function, efficient optimization, and multithreading. *J. Comput. Chem.* **31**, 455–461 (2010).

58. Z. Wang, H. Sun, X. Yao, D. Li, L. Xu, Y. Li, S. Tian, T. Hou, Comprehensive evaluation of ten docking programs on a diverse set of protein-ligand complexes: the prediction accuracy of sampling power and scoring power. *Phys. Chem. Chem. Phys.* **18**, 12964–12975 (2016).

59. E. Krieger, G. Koraimann, G. Vriend, Increasing the precision of comparative models with YASARA NOVA—A self-parameterizing force field. *Proteins* **47**, 393–402 (2002).

60. J. Poole, C. J. Day, T. Haselhorst, F. E. Jen, V. J. Torres, J. L. Edwards, M. P. Jennings, Repurposed Drugs That Block the Gonococcus-Complement Receptor 3 Interaction Can Prevent and Cure Gonococcal Infection of Primary Human Cervical Epithelial Cells. *mBio* **11**, e03046-19 (2020).

61. K. H. Gardner, L. E. Kay, The use of 2H, 13C, 15N multidimensional NMR to study the structure and dynamics of proteins. *Annu. Rev. Biophys. Biomol. Struct.* **27**, 357–406 (1998).

62. W. F. Vranken, W. Boucher, T. J. Stevens, R. H. Fogh, A. Pajon, M. Llinas, E. L. Ulrich, J. L. Markley, J. Ionides, E. D. Laue, The CCPN data model for NMR spectroscopy: development of a software pipeline. *Proteins* **59**, 687–696 (2005).

63. L. Xu, B. Huang, H. Du, X. C. Zhang, J. Xu, X. Li, Z. Rao, Crystal structure of cytotoxin protein suilysin from Streptococcus suis. *Protein Cell* **1**, 96–105 (2010).

Citation: L. K. Shewell, C. J. Day, F. E.-C. Jen, T. Haselhorst, J. M. Atack, J. F. Reijneveld, A. Everest-Dass, D. B. A. James, K. M. Boguslawski, S. Brouwer, C. M. Gillen, Z. Luo, B. Kobe, V. Nizet, M. von Itzstein, M. J. Walker, A. W. Paton, J. C. Paton, V. J. Torres, M. P. Jennings, All major cholesterol-dependent cytolysins use glycans as cellular receptors. *Sci. Adv.* **6**, eaaz4926 (2020).

Science Advances

All major cholesterol-dependent cytolysins use glycans as cellular receptors

Lucy K. Shewell, Christopher J. Day, Freda E.-C. Jen, Thomas Haselhorst, John M. Atack, Josephine F. Reijneveld, Arun Everest-Dass, David B. A. James, Kristina M. Boguslawski, Stephan Brouwer, Christine M. Gillen, Zhenyao Luo, Bostjan Kobe, Victor Nizet, Mark von Itzstein, Mark J. Walker, Adrienne W. Paton, James C. Paton, Victor J. Torres and Michael P. Jennings

ARTICLE TOOLS	http://advances.sciencemag.org/content/6/21/eaaz4926
SUPPLEMENTARY MATERIALS	http://advances.sciencemag.org/content/suppl/2020/05/18/6.21.eaaz4926.DC1
REFERENCES	This article cites 62 articles, 13 of which you can access for free http://advances.sciencemag.org/content/6/21/eaaz4926#BIBL
PERMISSIONS	http://www.sciencemag.org/help/reprints-and-permissions

Use of this article is subject to the Terms of Service